MINERALOGY AND PETROLOGY OF LASER IRRADIATED ARTIFICIAL CARBONACEOUS CHONDRITE: IMPLICATION TO THE MARTIAN MOONS AND SOME ASTEROIDS. T. V. Shingareva[1], A. T. Basilevsky[1], A.V. Fisenko[1], L. F. Semjonova[1], I.A Roshchina[1]; E. V. Guseva[2], N.N. Korotaeva[2]; [1]Vernadsky Institute, RAS, Moscow, 119991, Russia, shingareva@geokhi.ru; [2]Moscow State University, Russia.

Introduction: This work is devoted to the effects of micrometeorite impact melting of carbonaceous and ordinary chondrite materials that is relevant to space weathering of regolith on some asteroids and Martian moons. Following [1,2] we melted by laser pulses the artificial analog of CM chondrite (sample 1) and ordinary chondrite Tsarev (sample 2) and studied the experiment products under SEM and microprobe. The companion work considers VIS-IR spectra of the experiment products [3]. The micrometeorite impacts were simulated by irradiation of powdered (mostly to <30μm) samples under (2–3) x 10^{-4}mm Hg vacuum by the ND-YAG multiple-pulse laser (λ = 1.06μm) with impulse frequency 30–40 KHz. Pulse duration was 0.5–1 μsec, laser power ~1.2 KW and laser beam was ~100 μm wide).

The initial materials. The CM analog is a mixture of 46 mass % of non-magnetic fraction of L5 chondrite Tsarev, 47% of serpentine, 5% of kerite and 2% of calcite. Chemical compositions of the mixture and its main components are presented in the Table. Mineralogy of Tsarev is typical for meteorites of this class: silicates ~93% by vol. (olivine, orthopyroxene, clinopyroxene, plagioclase, glass); FeNi-metal, 3.5%, troilite, 2.5%, and chromite ~ 0.7 % [4].

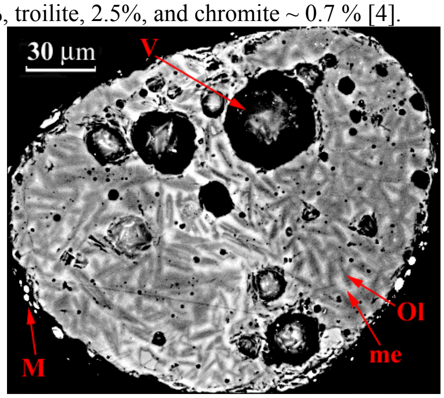

Fig.1. BSE image of CM simulant altered droplet: Ol – olivine, me – mesostasis, M – metal, V – vesicles.

The resulted products. After the laser treatment, samples were sieved into six size fractions: a) >300, b) 200-300, c) 125-200, d) 75-125, e) 40-75, and f) <40 μm. Fractions >125μm (a-c) contain mostly the altered material and were used for SEM and microprobe studies. Examination of altered material under binocular microscope showed that spherical glassy droplets of ~0.3 mm in diameter and their aggregates formed. The altered "mixture" products are generally opaque, black and their surfaces are enriched in circular drop-like metal/sulfide inclusions. The altered aggregates of Tsarev are grayish-green to black and generally opaque; their surfaces also show the metal/sulfide droplets, but in smaller amounts. All altered aggregates have unaltered powder grains stuck to their surfaces: the most contaminated with unaltered materials are fractions 1a, 2b-c, and the most free are 2a and 1b-c.

Mineralogy and petrology of altered samples. Chemistry analysis and BSE imaging of altered and initial samples were made at the Moscow State University Camebax SX 50 microprobe facility and SEM (CamScan 4 DV).

Sample 1 - "Mixture". The homogeneous grain size of the initial material has not been achieved, so some serpentine clasts are up to ~100 μm across, being coarser than the majority of the "mixture" clasts (≤ 30μm). Some of these large serpentine particles (~5% of the product) remained unmelted and welded to the melt droplets forming very porous contact zones. The melted material is partly crystallized forming intersertal texture (fig. 1) and *does not contain* the unmelted clasts in the droplet interiors but small unmelted clasts stuck to some droplet surfaces (up to 20%). Glassy droplets contain 12–20 vol. % of gas bubbles with sizes ranging from ~0.1 μm (the resolution limit) to 50-90 μm. The crystallization of the melt resulted in formation of skeletal, dendrite and needle-like Mg-rich (Fa=6.8 mole % on average) olivine (Ol) crystals with very thin (<1 μm) Fe-rich outer zones. The crystals 3-30 μm long and 1-7μm wide. They are cemented by glassy mesostasis, which occupies small areas between Ol-crystals. Within the analysis error bars, the mean bulk chemistry of the melt (Ol+mesostasis) is similar to that of the initial material except of some depletion in FeO. The melt is compositionally heterogeneous showing brighter and darker areas on BSE images (Fig. 1). Relative to the initial material "dark" melt shows enrichment in SiO_2 and MgO and slightly in CaO and Al_2O_3 and striking depletion in FeO (Table). It consists of Ol (80% by area) and the pyroxene composition mesostasis (20%). "Bright" melt contains more FeO than the initial material and is slightly depleted in SiO_2. Apparently the melt heterogeneity is due to closeness of the laser beam diameter and size of the largest serpentine particles. Many fine (0.1–0.5 μm) Fe-rich inclusions dispersed in mesostasis and many circular metal/sulfide inclusions (<1 to 10 μm in dia) are seen on the melt droplet surface. Similar inclusions are seen also on the inner surfaces of large pores in melt/unmelted material contacts. Rather large (up to 15μm) troilite-metal inclusions are seen in some melt droplets (up to 2% of their volume).

Sample 2 -Tsarev. Laser heating *did not lead to complete melting* of Sample 2. Altered aggregates of this sample contain from 6 to 13% of unmelted angular clasts (3-100 μm in length) cemented by melt. The melt consists of intersertal mixture of compositionally zoned (Fe-rich rims) skeletal to filamentous olivine crystals (8 to 60 μm long and 2 to 6 μm wide) and mesostasis (Fig. 2). The melt contains 5–15% of gas bubbles from ~0.1 to 70-130 μm in diameter and large (up to 50 μm) metal/sulfide droplets (immiscibility effect?).

If to ignore the metal/sulfide droplets, the melt is slightly enriched in SiO_2 and depleted in FeO relative to the initial material (Table). Mesostasis is enriched in Fe and in some its parts has the pyroxene composition. The metal/sulfide inclusions (up to 4% by area) are concentrated on the edges of the melt droplets, being are disseminated in the groundmass.

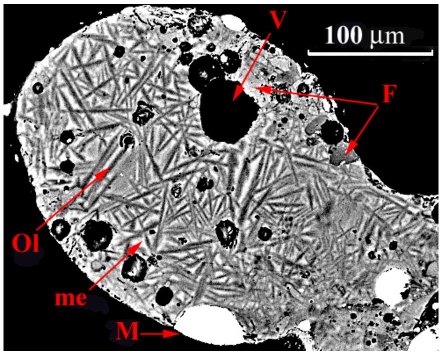

Fig.2. BSE image of Tsarev melt droplet: Ol – olivine, me – mesostasis, F –unfused fragments, M – metal, V – vesicles

Discussion and conclusions. The laser pulse irradiation of the CM chondrite simulant and L5 chondrite Tsarev led to local melting, formation of the melt droplets and their partial crystallization: compositionally zoned (Fe-enriched outer parts) skeletal to filamentous olivine crystals and glass formed. Metal/sulfide phases segregated mostly in the outer parts of the melt droplets. The volatile components (H_2O of serpentine and CO_2 of calcite) have undoubtedly escaped from the melting products. The micrometeorite bombardment of the carbonaceous and ordinary chondrite materials should obviously lead to similar results. Some of these effects (e.g., dehydration and apparent changing of Fe/Mg ratio due to formation of zoned Ol crystals), if occur on asteroids and Martian satellites, can be noticed by the remote sensing.

The experiments showed that comparing to Tsarev, the CM simulant is more susceptible to laser pulse melting despite that at λ= 1.06 µm the simulant is even more reflective than Tsarev [3]. In this process, volatiles escape, seemingly playing no role in the melting, which effectiveness is probably controlled by the composition of nonvolatile components. If the carbonaceous chondrites comparing to the ordinary ones are more susceptible to impact melting too, then the regolith of parent bodies of the firsts can be more susceptible to this side of space weathering than the regolith of the seconds.

Acknowledgment: The work was supported by RFBR grant 02-05-65156.

References: [1] Moroz et.al. (1996) *Icarus*, 122, 366–382. [2] Basilevsky et al. (2000) *Geochemistry International*, 38, Suppl. 3, S390–S403. [3] Hiroi et al. (2003) *LPSC 34 Abs*, this CD. [4] Semenenko & Samojlovich (1982) *Meteoritika*, 41, 31–36 (in Russian).

Table 1 Chemical composition of initial material[a] and melted products[b]. ([a]XRF analyses, Vernadsky Institute; [b]microprobe analyses, Moscow State University).

	Unaltered materials					Altered materials					
	Tsarev	Serpentine		"Mixture"		Sample 1 products					Sample2 prods.
		With LOI	LOI free	With LOI	LOI free	Bulk "melt" mean	Bulk "melt" "bright"	Bulk "melt" "dark"	Ol cryst.	Mesostasis	Bulk "melt"
SiO_2	44.84	40.71	47.26	39.24	44.28	45.4	42.5	48.3	42.3	52.3	46.8
TiO_2	0.14	0.02	0.02	0.08	0.09	0.1	0.1	0.1	0	0.1	0.2
Al_2O_3	2.56	0.48	0.56	1.43	1.61	1.9	1.6	2.2	0.1	3.8	2.9
FeO	20.95	4.73	5.49	13.54	15.28	12.7	17.8	7.6	6.5	17.3	17.7
MnO	0.36	0.04	0.05	0.19	0.21	0.3	0.2	0.3	0.2	0.4	0.4
MgO	27.86	39.67	46.05	31.45	35.50	36.4	35.1	37.7	50.3	17.2	27.9
CaO	1.97	<0.01	<0.01	1.93	2.18	2.4	1.9	2.8	0.3	7.1	2.3
Na_2O	<0.01	<0.01	<0.01	<0.01	<0.01	b.d.	b.d.	b.d.	b.d	b.d.	0.7
K_2O	0.15	<0.01	<0.01	0.04	0.05	b.d.	b.d.	b.d.	b.d	b.d	0.2
P_2O_5	0.48	0.03	0.03	0.23	0.26	0.3	0.7	b.d.	b.d.	b.d	0.5
Cr_2O_3	0.62	0.43	0.51	0.47	0.53	0.4	b.d.	0.9	0.3	0.9	0.2
S	n.d,	n.d.	n.d.	n.d.	n.d.	0.1	0.1	0.1	b.d	0.9	0.2
Σ	99.94	86.14	100.0	88.61	100.0	100.0	100.0	100.0	100.0	100.0	100.0
LOI		12.98		10.92							
Σ_{LOI}		99.12		99.53							
MG#	70.3		93.7		80.5	83.6	77.8	89.8	93.2	63.9	73.7